EUROFUSION WP15ER-PR(16) 16618

C. Wersal et al.

A comparison between a refined two-point model for the limited tokamak SOL and self-consistent plasma turbulence simulations

Preprint of Paper to be submitted for publication in
Plasma Physics and Controlled Fusion

This work has been carried out within the framework of the EUROfusion Consortium and has received funding from the Euratom research and training programme 2014-2018 under grant agreement No 633053. The views and opinions expressed herein do not necessarily reflect those of the European Commission.

A comparison between a refined two-point model for the limited tokamak SOL and self-consistent plasma turbulence simulations

C. Wersal, P. Ricci

September 30, 2016

Abstract

A refined two-point model is derived from the drift-reduced Braginskii equations for the limited tokamak scrape-off layer (SOL). It balances the parallel plasma dynamics, the plasma-neutral interaction, and the radial plasma and heat transport from the tokamak core. Self-consistent first-principle turbulence simulations of the SOL plasma including its interaction with neutral atoms are perfomed with the GBS code and compared to the refined two-point model and a simple version. The refined two-point model is shown to

be in very good agreement with the turbulence simulation results.

1 Introduction

The level of impurities in the core and the lifetime of the plasma facing components, two critical issues on the way to fusion energy, depend on the amount of sputtering of wall material [9]. Sputtering occurs when ions, accelerated in the sheath, hit the solid wall. The acceleration is directly related to the plasma temperature in front of the divertor or limiter plates [16]. Therefore, understanding the physical processes that regulate the plasma temperature in front of the solid walls is of paramount importance.

Reliable predictions of the conditions in front of the solid walls can be obtained by using three-dimensional simulations of the turbulent dynamics in the outermost plasma region of a fusion device, the scrape-off layer (SOL). A number of simulation codes were developed in the past years to carry out these simulations, such as BOUT++ [4], GBS [13, 6], GRILLIX [18], and TOKAM3X [19]. However, their development is still ongoing and turbulence simulations remain computationally very expensive. For this reason, progress was made in the development of simplified models that describe

perpendicular turbulent transport as a diffusive process with diffusion coefficients obtained from fitting experimental data. Widely used transport codes that use these models are, e.g., SOLEDGE2D-EIRENE [3], SOLPS formerly B2-EIRENE [11, 15, 12], EMC3-EIRENE [5], UEDGE [14]. Further simplifications of these transport models lead to the so-called two-point models [16], which are widely used to obtain fast, although rough, estimates of plasma parameters in front of the solid walls. Two-point models can be used to understand basic trends of the parallel transport in the tokamak SOL. Two-point models use assumptions about the perpendicular heat and particle fluxes and a one-dimensional description of the plasma dynamics along the field lines to obtain relations between the plasma parameters at the target (the divertor or limiter plates) and upstream (a location far from the target and in contact with the core, e.g., close to the X-point, where the divertor legs begin, or at the low-field side midplane). While a number of two-point models were developed in the past varying in their geometries, assumptions, and inclusion of different physical processes (see, e.g., Refs. [17, 20, 7, 16]), to our knowledge no direct comparison of two-point models with the results of turbulence codes was carried out. The goal of the present paper is to perform such a comparison by evaluating the electron temperature drop from the up-

stream to the target regions in a very simple magnetic configuration, i.e. a tokamak with a toroidal limiter on the high-field side equatorial midplane with circular magnetic flux surfaces. In this case, the targets are the lower and upper sides of the limiter, while the upstream location is at the low-field side equatorial midplane, halfway between the two targets.

Since in the limited configuration the target location is next to the confined region a large fraction of the recycled neutral atoms are ionized inside the confined region, even in high density plasmas, where the ionization mean free path is short. The plasma can redistribute itself poloidally in the closed flux surface region, by moving along the magnetic field lines, and it flows back out to the SOL also at locations far from the limiter. Therefore, plasma parallel flows towards the limiter are important and, contrary to what is often done for high-density divertor configurations [16], the parallel convective heat flux cannot be neglected. It turns out that the simplest two-point model in limited configuration is derived from the balance between perpendicular heat transport, parallel heat conduction, and parallel heat convection [20]. In the present paper, we compare the predictions of this model to first-principle turbulence simulations carried out with the GBS code. Since the comparison is not completely satisfactory, we derive a more refined two-point model

rigorously from the fluid drift-reduced Braginskii equations that are coupled to a kinetic equation for neutral atoms. The comparison of this model with the turbulence simulations shows good agreement.

The present paper is structured as follows. After the Introduction, in Sec. 2 we describe a simple two-point model for toroidally limited tokamaks. Sec. 3 compares the prediction of this model with the SOL turbulence simulations. In Sec. 4 we develop a more accurate two-point model, which we compare to the turbulent simulations and discuss in Sec. 5.

2 A simple two-point model for the limited SOL

In this chapter we describe a simple two-point model for an axi-symmetric tokamak with a toroidal limiter. We consider one flux tube, which spans along a magnetic the field line from one side to the other side of the limiter. We assume that the limiter is located at the high-field side equatorial midplane. We label the direction along the flux tube with the coordinate s, which spans from $s = -L$ at the lower side of the limiter, to $s = +L$ at its upper side, with the upstream location, $s = 0$, located at the low-field side

equatorial midplane. We remark that all flux tubes on the same flux surface show equal behavior, since we consider an axi-symmetric system.

Since in the limited configuration the target location is next to the confined region, a large fraction of the recycled neutral atoms is ionized, even in high density plasmas, inside the closed flux surface region, where the ionized particles can redistribute poloidally. The flow of particles into the SOL is poloidally constant to a first approximation. As a consequence, large plasma flows towards the limiter are present and the parallel convective heat flux cannot be neglected. The simplest two-point model in limited configuration [20] is derived from the balance between the heat deposited in the flux tube due to the radial heat transport, $S_{Q\perp}$, the parallel heat conduction, Q_{cond}, and the parallel heat convection, Q_{conv}, i.e.

$$Q_{cond}(s) + Q_{conv}(s) = \int_0^s S_{Q\perp}(s')ds'. \tag{1}$$

In Eq. (1) we impose $Q_{cond}(0) = Q_{conv}(0) = 0$ because the upstream location, $s = 0$, is both a symmetry and a stagnation point in this simple model. The conductive heat flux is modeled by using the Spitzer heat flux coefficient, $Q_{cond} = -\chi_{e0} T_e^{5/2} dT_e/ds$, and the convective heat flux is estimated with $Q_{conv} = c_{e0}\Gamma T_e$, where $c_{e0} = 5/2$ is the heat capacity of the electrons and $\Gamma = \int S_{n\perp} ds$ is the parallel particle flux, with $S_{n\perp}$ being the particle source

due to radial transport into the flux tube. Assuming $S_{Q\perp}$ and $S_{n\perp}$ constant along the flux tube in a limited geometry (the outflow of plasma and heat is poloidally uniform), the equation that determines the electron temperature is

$$-\chi_{e0} T_e^{5/2} \frac{dT_e}{ds} + c_{e0} s S_{n\perp} T_e = s S_{Q\perp}. \tag{2}$$

The solution of Eq. (2) requires a boundary condition that we apply at the magnetic pre-sheath entrance by writing the electron heat flux through the sheath entrance as $Q_t = \gamma_e \Gamma_t T_{e,t}$, where the subscript t indicates the target location, and the coefficient $\gamma_e \approx 5$ is the electron sheath transmission coefficient [16].

With this boundary condition Eq. (2) can be integrated numerically for a given $S_{Q\perp}$ and $S_{n\perp}$. An implicit analytical expression to relate the electron temperature at the target, $T_{e,t}$ to its upstream value $T_{e,u}$ can also be obtained [20] that can be evaluated numerically.

3 Turbulent SOL simulations and comparison with the simple two-point model

In this section we introduce the model that we use to describe plasma turbulence in the tokamak SOL and its interaction with neutrals, by outlining the basic assumptions of the model and presenting the resulting equations. (A more complete derivation can be found in Refs. [22, 21].) The electron temperature drop from the upstream to the target location predicted by this model, which is implemented in the GBS code [13, 6], is then compared with the simple two-point model.

Since the plasma in the SOL is rather cold (a few eV), its collisionality is sufficiently high that a fluid model, such as Braginskii's model [2], can be used for its description. Moreover, by taking advantage of the fact that plasma turbulence is elongated along the field lines ($k_\parallel \ll k_\perp$) and that turbulent timescales are much slower than the ion cyclotron motion ($\partial/\partial t \ll \Omega_{ci}$) the drift reduction can be applied [22]. This leads, together with quasi-neutrality, to a set of drift-reduced two-fluid Braginskii equations that describe the dynamics of plasma density, n, generalized vorticity, $\tilde{\omega}$, electron and ion parallel velocities, $v_{\parallel \mathrm{e}}$ and $v_{\parallel \mathrm{i}}$, and electron and ion temperatures, T_e and T_i.

In the electrostatic limit these equations are

$$\frac{\partial n}{\partial t} = -\frac{1}{B}[\phi, n] - \nabla_\parallel(n v_{\parallel \mathrm{e}}) + \frac{2}{eB}\left[C(p_\mathrm{e}) - enC(\phi)\right] + \mathcal{D}_\mathrm{n}(n) + S_\mathrm{n} \tag{3}$$

$$+ n_\mathrm{n}\nu_\mathrm{iz} - n\nu_\mathrm{rec}$$

$$\frac{\partial \tilde{\omega}}{\partial t} = -\frac{1}{B}[\phi, \tilde{\omega}] - v_{\parallel \mathrm{i}}\nabla_\parallel \tilde{\omega} + \frac{B^2}{m_\mathrm{i} n}\nabla_\parallel j_\parallel + \frac{2B}{m_\mathrm{i} n}C(p) + \mathcal{D}_{\tilde{\omega}}(\tilde{\omega}) - \frac{n_\mathrm{n}}{n}\nu_\mathrm{cx}\tilde{\omega} \tag{4}$$

$$\frac{\partial v_{\parallel \mathrm{e}}}{\partial t} = -\frac{1}{B}[\phi, v_{\parallel \mathrm{e}}] - v_{\parallel \mathrm{e}}\nabla_\parallel v_{\parallel \mathrm{e}} + \frac{e}{\sigma_\parallel m_\mathrm{e}} j_\parallel \tag{5}$$

$$+ \frac{e}{m_\mathrm{e}}\nabla_\parallel \phi - \frac{T_\mathrm{e}}{m_\mathrm{e} n}\nabla_\parallel n - \frac{1.71}{m_\mathrm{e}}\nabla_\parallel T_\mathrm{e} + \mathcal{D}_{v_{\parallel \mathrm{e}}}(v_{\parallel \mathrm{e}})$$

$$+ \frac{n_\mathrm{n}}{n}(\nu_\mathrm{en} + 2\nu_\mathrm{iz})(v_{\parallel \mathrm{n}} - v_{\parallel \mathrm{e}})$$

$$\frac{\partial v_{\parallel \mathrm{i}}}{\partial t} = -\frac{1}{B}[\phi, v_{\parallel \mathrm{i}}] - v_{\parallel \mathrm{i}}\nabla_\parallel v_{\parallel \mathrm{i}} - \frac{1}{m_\mathrm{i} n}\nabla_\parallel p + \mathcal{D}_{v_{\parallel \mathrm{i}}}(v_{\parallel \mathrm{i}}) \tag{6}$$

$$+ \frac{n_\mathrm{n}}{n}(\nu_\mathrm{iz} + \nu_\mathrm{cx})(v_{\parallel \mathrm{n}} - v_{\parallel \mathrm{i}})$$

$$\frac{\partial T_\mathrm{e}}{\partial t} = -\frac{1}{B}[\phi, T_\mathrm{e}] - v_{\parallel \mathrm{e}}\nabla_\parallel T_\mathrm{e} + \frac{4T_\mathrm{e}}{3eB}\left[\frac{T_\mathrm{e}}{n}C(n) + \frac{7}{2}C(T_\mathrm{e}) - eC(\phi)\right] \tag{7}$$

$$+ \frac{2T_\mathrm{e}}{3n}\left[\frac{0.71}{e}\nabla_\parallel j_\parallel - n\nabla_\parallel v_{\parallel \mathrm{e}}\right] + \mathcal{D}_{T_\mathrm{e}}(T_\mathrm{e}) + \kappa_{\parallel \mathrm{e}}\nabla_\parallel(T_\mathrm{e}^{5/2}\nabla_\parallel T_\mathrm{e}) + S_{T_\mathrm{e}}$$

$$+ \frac{n_\mathrm{n}}{n}\nu_\mathrm{iz}\left[-\frac{2}{3}E_\mathrm{iz} - T_\mathrm{e} + m_\mathrm{e} v_{\parallel \mathrm{e}}\left(v_{\parallel \mathrm{e}} - \frac{4}{3}v_{\parallel \mathrm{n}}\right)\right] - \frac{n_\mathrm{n}}{n}\nu_\mathrm{en} m_\mathrm{e}\frac{2}{3}v_{\parallel \mathrm{e}}(v_{\parallel \mathrm{n}} - v_{\parallel \mathrm{e}})$$

$$\frac{\partial T_\mathrm{i}}{\partial t} = -\frac{1}{B}[\phi, T_\mathrm{i}] - v_{\parallel \mathrm{i}}\nabla_\parallel T_\mathrm{i} + \frac{4T_\mathrm{i}}{3eB}\left[C(T_\mathrm{e}) + \frac{T_\mathrm{e}}{n}C(n) - \frac{5}{2}C(T_\mathrm{i}) - eC(\phi)\right] \tag{8}$$

$$+ \frac{2T_\mathrm{i}}{3n}\left[\frac{1}{e}\nabla_\parallel j_\parallel - n\nabla_\parallel v_{\parallel \mathrm{i}}\right] + \mathcal{D}_{T_\mathrm{i}}(T_\mathrm{i}) + \kappa_{\parallel \mathrm{i}}\nabla_\parallel(T_\mathrm{i}^{5/2}\nabla_\parallel T_\mathrm{i}) + S_{T_\mathrm{i}}$$

$$+ \frac{n_\mathrm{n}}{n}(\nu_\mathrm{iz} + \nu_\mathrm{cx})\left[T_\mathrm{n} - T_\mathrm{i} + \frac{1}{3}(v_{\parallel \mathrm{n}} - v_{\parallel \mathrm{i}})^2\right]$$

with $p = n(T_\mathrm{e} + T_\mathrm{i})$, the total pressure, $j_\parallel = en(v_{\parallel\mathrm{i}} - v_{\parallel\mathrm{e}})$, $\kappa_{\parallel\mathrm{e}}$ and $\kappa_{\parallel\mathrm{i}}$ the Spitzer heat conduction coefficients, E_iz the effective ionization energy, and $\sigma_\parallel = 1.96e^2 n\tau_\mathrm{e}/m_\mathrm{e}$, the parallel conductivity, where τ_e is the electron collision time. The generalized vorticity, $\tilde{\omega} = \omega + 1/e\nabla_\perp^2 T_\mathrm{i}$, is related to the electrostatic potential by $\nabla_\perp^2\phi = \omega$. The following operators are used $\nabla_\parallel A = \hat{\mathbf{b}}\cdot\nabla A$, $[A,B] = \hat{\mathbf{b}}\cdot(\nabla A\times\nabla B)$, and $C(A) = B/2[\nabla\times(\hat{\mathbf{b}}/B)]\cdot\nabla A$. The source terms ($S_n$, S_{T_e}, S_{T_i}) mimic the outflow of hot plasma from the confined region to the SOL, and we interpret their location as the radial position of the last closed flux surface (LCFS). The perpendicular diffusive terms $\mathcal{D}_A(A)$ are included mostly for numerical reasons. The system is closed by a set of first-principles boundary conditions applied at the magnetic pre-sheath entrance of the limiter plates, derived and discussed in Ref. [10].

The interaction of the plasma with the neutral atoms, rigorously deduced from a kinetic description [21], is included through the interaction with the neutral density, n_n, parallel velocity, $v_{\parallel\mathrm{n}}$, and temperature, T_n. These moments of the neutral distribution function are obtained from the solution of the kinetic neutral equation for a mono-atomic neutral species

$$\frac{\partial f_\mathrm{n}}{\partial t} + \mathbf{v}\cdot\frac{\partial f_\mathrm{n}}{\partial \mathbf{x}} = -\nu_\mathrm{iz} f_\mathrm{n} - \nu_\mathrm{cx}\left(f_\mathrm{n} - \frac{n_\mathrm{n}}{n_\mathrm{i}} f_\mathrm{i}\right) + \nu_\mathrm{rec} f_\mathrm{i} \tag{9}$$

where f_n and f_i are the neutral and ion distribution functions. The ion-

ization, charge-exchange, and recombination processes are described, respectively, through the use of Krook operators with collision frequencies defined as $\nu_{\rm iz} = n_{\rm e}\langle v_{\rm e}\sigma_{\rm iz}(v_{\rm e})\rangle$, $\nu_{\rm rec} = n_{\rm e}\langle v_{\rm e}\sigma_{\rm rec}(v_{\rm e})\rangle$, and $\nu_{\rm cx} = n_{\rm i}\langle v_{\rm i}\sigma_{\rm cx}(v_{\rm i})\rangle$, where $\sigma_{\rm iz}$, $\sigma_{\rm rec}$, and $\sigma_{\rm cx}$ are the ionization, recombination, and charge-exchange cross sections. (The $\langle\cdot\rangle$ operator denotes the averaging over the Maxwellian electron, or ion, distribution function.) Eqs. (3-8) are solved by the GBS code by using a second order finite difference scheme, except for the $[A, B]$ operators that are discretized by using the Arakawa scheme [1]. Time integration is carried out with the classical Runge-Kutta method [8]. The solution of Eq. (9) is obtained in the limit of $\tau_{\rm n} < \tau_{\rm turb}$ ($\tau_{\rm n}$ is the mean flight time of a neutral atom, $\tau_{\rm turb}$ is the turbulent timescale) and $k_\parallel < \lambda_{\rm mfp}$ ($\lambda_{\rm mfp}$ is the mean free path of the neutrals) by using the method of characteristics [21].

To compare the simple two-point model with results from the GBS code, we consider five simulations, with a toroidal limiter on the high-field equatorial midplane, $R/\rho_{\rm s0} = 500$, $m_{\rm i}/m_{\rm e} = 400$, $2\pi a = 800\rho_{\rm s0}$, a being the minor radius, $\rho_{\rm s0} = c_{\rm s0}/\Omega_{\rm ci}$, $c_{\rm s0} = \sqrt{T_{\rm e0}/m_{\rm i}}$, and $T_{\rm e0} = T_{\rm i0} = 10$eV. The five simulations are variants of two basic configurations, characterized by two different plasma densities, which were also used in Ref. [21]. In the low plasma density configuration, we impose $n_0 = 5 \cdot 10^{18}{\rm m}^{-3}$, the value of the

density at the LCFS, and $\tilde{\nu} = Rm_{\rm e}/(1.96c_{\rm s0}m_{\rm i}\tau_{\rm e}) = 0.02$, the resistivity normalized to $R/c_{\rm s0}$. As a consequence, the dimensionless parallel electron heat conductivity is $\tilde{\kappa}_{\parallel {\rm e}} = 3.16 \times 2T_{\rm e0}\tau_{\rm e}/(3m_{\rm e}c_{\rm s0}R) = 56.0$, and the dimensionless parallel ion heat conductivity is $\tilde{\kappa}_{\parallel {\rm i}} = 3.9 \times 2T_{\rm i0}\tau_{\rm i}/(3m_{\rm i}c_{\rm s0}R) = 1.6$. In the high plasma density configuration, $n_0 = 5 \cdot 10^{19}{\rm m}^{-3}$, $\tilde{\nu} = 0.2$, $\tilde{\kappa}_{\parallel {\rm e}} = 5.6$, and $\tilde{\kappa}_{\parallel {\rm i}} = 0.16$ are used. In addition to these two basic simulations, we repeat both simulations zeroing out the plasma interaction terms with the neutral atoms. These simulations are labeled as 'no n_n' in the following. For the high density case, we also carry out a simulation where we change the energy removed by each ionization to include the increased energy loss due to multiple impact ionizations, labeled as '$E_{iz} = 30$eV' (in the other cases $E_{iz} = 13.6$eV). The computational domain extends for all five simulations from $r_{\rm min} = 0$ to $r_{\rm max} = 150\rho_{\rm s0}$. The source terms $S_{\rm n}$, $S_{T_{\rm i}}$, and $S_{T_{\rm e}}$ in Eqs. (3-8) are constant in time, poloidally uniform, and radially Gaussian around $r_{\rm s} = 30\rho_{\rm s0}$ with a width of $5\rho_{\rm s0}$.

The comparison with the simple two-point model is performed for five different flux tubes extending radially over $10\rho_{\rm s0}$ centered at $r = 45, 55, 65, 75, 85\rho_{\rm s0}$. To calculate the particle and heat deposited into each flux tube, $S_{n\perp}$ and $S_{Q\perp}$, we combine the perpendicular drift terms in the GBS equations (as explained

in Sec. 4), and we average them over time and over the poloidal direction.

The two-point model estimates of the temperature ratio, $T_{\mathrm{e,u}}/T_{\mathrm{e,t}}$, are then compared to the temperature ratio in the simulations. The results are shown in Fig. 1. While the general trends are captured by the simple two-point model, the agreement with the turbulent simulations is rather poor in most cases.

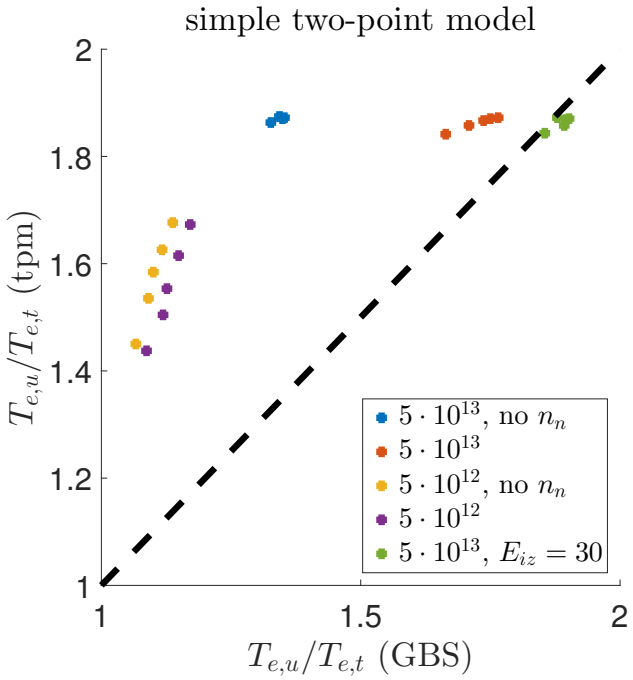

Figure 1: Comparison of the ratio between the electron temperature at the upstream and target locations predicted by the simple two-point model (tpm), Eq. (2), with the results of a set of GBS simulations. For each simulation (different colors) we consider five radial locations for the flux tube ($r = 45, 55, 65, 75, 85\rho_{s0}$).

4 A refined two-point model for limited SOL

In this chapter, we derive a refined two-point model rigorously from the drift-reduced Braginskii equations for plasma density, Eq. (3), and electron

temperature, Eq. (7). The perpendicular diffusive terms, $\mathcal{D}_n(n)$ and $\mathcal{D}_{T_\mathrm{e}}(T_\mathrm{e})$, included mostly for numerical reasons, are neglected, since they are small. For typical parameters of limited tokamaks, the SOL plasma temperature is sufficiently high to neglect recombination processes. Furthermore, we neglect the terms in the electron temperature equation (7) associated with the difference between parallel electron and neutral velocity since they are small compared to the other plasma-neutral interaction terms. We also assume $j_\parallel = 0$. The validity of these assumptions is shown in Fig. 2. By making use of these assumptions, we obtain

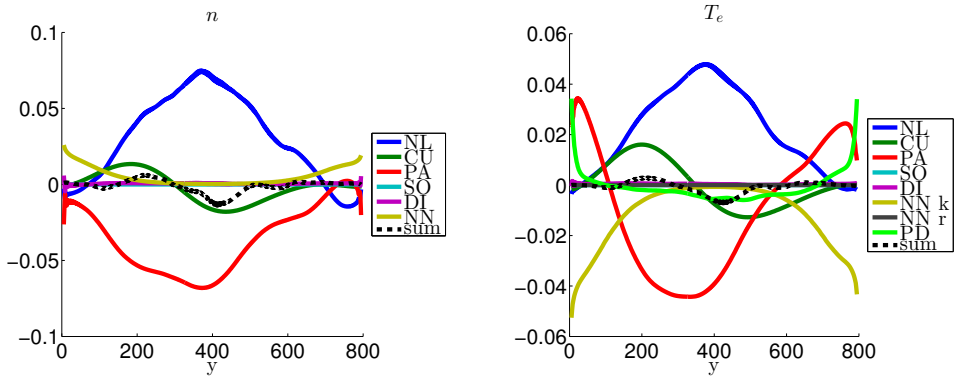

Figure 2: Time-averaged plasma density (left) and electron temperature (right) balance along the field lines between the two limiter plates. The contributions are labeled NL, for the ExB term, CU, for the curvature term, PA, for the parallel flow, SO, for the source term, DI, for the perpendicular numerical diffusion, NN, for the neutrals, where k marks terms that are kept, and r terms that are neglected, and PD the parallel conduction. The sum in black shows that the quasi steady state balance is almost exact.

$$\frac{\partial n}{\partial t} + \nabla_\parallel (n v_{\parallel \mathrm{e}}) = \tilde{S}_{\mathrm{n}\perp} + \tilde{S}_{\mathrm{n}\perp n_\mathrm{n}} \tag{10}$$

$$\frac{\partial T_\mathrm{e}}{\partial t} + v_{\parallel \mathrm{e}} \nabla_\parallel T_\mathrm{e} + \frac{2T_\mathrm{e}}{3} \nabla_\parallel v_{\parallel \mathrm{e}} - \kappa_\mathrm{e} \nabla_\parallel (T_\mathrm{e}^{5/2} \nabla_\parallel T_\mathrm{e}) = \tilde{S}_{T_\mathrm{e}\perp} + \tilde{S}_{T_\mathrm{e}\perp n_\mathrm{n}} \tag{11}$$

where we combine the perpendicular transport terms (the terms related to the $\mathbf{E} \times \mathbf{B}$ and diamagnetic drifts as well as the S_n and S_{T_e} terms) into

effective perpendicular source terms,

$$\tilde{S}_{\mathrm{n}\perp} = -\frac{1}{B}[\phi, n] + \frac{2}{eB}\left[C(p_{\mathrm{e}}) - enC(\phi)\right] + S_{\mathrm{n}} \tag{12}$$

$$\tilde{S}_{T_{\mathrm{e}}\perp} = -\frac{1}{B}[\phi, T_{\mathrm{e}}] + \frac{4T_{\mathrm{e}}}{3eB}\left[\frac{T_{\mathrm{e}}}{n}C(n) + \frac{7}{2}C(T_{\mathrm{e}}) - eC(\phi)\right] + S_{T_{\mathrm{e}}}, \tag{13}$$

and we do the same for the plasma-neutral interactions terms:

$$\tilde{S}_{\mathrm{n}\perp n_{\mathrm{n}}} = n_{\mathrm{n}}\nu_{\mathrm{iz}} \tag{14}$$

$$\tilde{S}_{T_{\mathrm{e}}\perp n_{\mathrm{n}}} = \frac{n_{\mathrm{n}}}{n}\nu_{\mathrm{iz}}\left(-\frac{2}{3}E_{\mathrm{iz}} - T_{\mathrm{e}}\right). \tag{15}$$

To obtain an equation for the parallel electron heat flux, we multiply Eq. (10) by $3T_e/2$, and Eq. (11) by $3n/2$ and we add the two resulting equations:

$$\frac{3}{2}\frac{\partial(nT_{\mathrm{e}})}{\partial t} + \frac{3}{2}T_{\mathrm{e}}\nabla_{\parallel}(nv_{\parallel\mathrm{e}}) + \frac{3}{2}nv_{\parallel\mathrm{e}}\nabla_{\parallel}T_{\mathrm{e}} + nT_{\mathrm{e}}\nabla_{\parallel}v_{\parallel\mathrm{e}} - \frac{3}{2}n\kappa_{\mathrm{e}}\nabla_{\parallel}(T_{\mathrm{e}}^{5/2}\nabla_{\parallel}T_{\mathrm{e}}) \tag{16}$$

$$= \frac{3}{2}T_{\mathrm{e}}\tilde{S}_{\mathrm{n}\perp} + \frac{3}{2}n\tilde{S}_{T_{\mathrm{e}}\perp} + \frac{3}{2}T_{\mathrm{e}}\tilde{S}_{\mathrm{n}\perp n_{\mathrm{n}}} + \frac{3}{2}n\tilde{S}_{T_{\mathrm{e}}\perp n_{\mathrm{n}}}.$$

We now average Eqs. (10) and (16) in time (and rearrange the terms) to obtain

$$\nabla_{\parallel}\left(nv_{\parallel\mathrm{e}}\right) \approx S_{\mathrm{n}\perp} + S_{\mathrm{n}\perp n_{\mathrm{n}}} \tag{17}$$

$$\nabla_{\parallel}\left(\frac{5}{2}nv_{\parallel\mathrm{e}}T_{\mathrm{e}}\right) - v_{\parallel\mathrm{e}}\nabla_{\parallel}\left(nT_{\mathrm{e}}\right) - \chi_{\mathrm{e}}\nabla_{\parallel}\left(T_{\mathrm{e}}^{5/2}\nabla_{\parallel}T_{\mathrm{e}}\right) \approx S_{Q\perp} - S_{\mathrm{n}\perp n_{\mathrm{n}}}E_{\mathrm{iz}}, \tag{18}$$

with $S_{\mathrm{n}\perp}$ and $S_{Q\perp}$ being the time average of $\tilde{S}_{\mathrm{n}\perp}$ and $3/2(T_{\mathrm{e}}\tilde{S}_{\mathrm{n}\perp} + n\tilde{S}_{T_{\mathrm{e}}\perp})$ respectively, and all quantities in Eqs. (17-18) meant to be time averaged. We note that the contribution due to the correlation between the fluctuations is small and can be neglected when time-averaging the parallel transport terms and the neutral-plasma interaction terms. Moreover, the coefficient in the parallel Spitzer heat conductivity is defined as $\chi_{\mathrm{e}} = \frac{3}{2} n_{\mathrm{ft}} \kappa_{\mathrm{e}}$, where n_{ft} is the average density in the flux tube.

To derive the electron temperature drop along the field lines from Eq. (18), we estimate the variation of the parallel electron velocity, the plasma density, and the neutral density along the field line. We assume that the parallel velocity varies linearly between the two limiters, where Bohm boundary conditions are valid, i.e.

$$v_{\parallel \mathrm{e}}(\pm L) = \pm c_{\mathrm{s}} = \pm \sqrt{\frac{T_{\mathrm{e}} + T_{\mathrm{i}}}{m_{\mathrm{i}}}} \approx \pm \sqrt{\frac{2T_{\mathrm{e}}}{m_{\mathrm{i}}}}. \tag{19}$$

obtaining therefore

$$v_{\parallel \mathrm{e}}(s) = \frac{c_s s}{L}. \tag{20}$$

To obtain the density profile, we integrate Eq. (17), that is

$$\Gamma = n v_{\parallel \mathrm{e}} = \int S_{\mathrm{n}\perp} + S_{\mathrm{n}\perp n_{\mathrm{n}}} ds. \tag{21}$$

The profile of the plasma density is then $n = \Gamma / v_{\parallel \mathrm{e}}$.

The neutral density is assumed to decay exponentially from the two limiters, i.e.

$$n_n(s) = n_n(-L) \exp\left[(-s - L)/\lambda_{\mathrm{mfp}}\right] + n_n(L) \exp\left[(s - L)/\lambda_{\mathrm{mfp}}\right], \qquad (22)$$

with the decaying scale length given by $\lambda_{\mathrm{mfp}} = \alpha_r c_s / (\nu_{\mathrm{iz}} + \nu_{\mathrm{cx}})$, where α_r is the reflection coefficient of the neutrals on the limiter [21] (the velocity of the thermal neutrals from the wall is much smaller and can be neglected when estimating the effective mean free path). The collision frequencies ν_{iz} and ν_{cx} are evaluated with the electron temperature and plasma density averaged around the target (from the limiter to a distance λ_{mfp} from the limiter). The target density, $n_n(\pm L)$, is chosen to match the total amount of ionization in the considered flux tube. This is an input for an one-dimensional model, since neutral particles are not bound to flow along a field line, and can, in the limited configuration, move easily accross the flux surfaces before being ionized. The ionization inside each flux tube amounts for about 5% to 20% of the recycled particles at its ends, depending mainly on plasma density and radial location of the considered flux tube. The perpendicular source terms, S_{n} and S_Q, are approximated to have a cosine distribution due to the ballooning character of the perpendicular transport, which is confirmed by

the turbulence simulations.

Finally, to solve (18) for the electron temperature, we impose symmetry around the upstream location $s = 0$, where the parallel derivative of T_e vanishes. We also ensure that the velocity profile is self-consistently evaluated with $T_e(\pm L)$ by enforcing that the integral of the parallel electron heat equation, Eq. (18), along s, i.e.

$$\begin{aligned}\left[\frac{5}{2}nv_{\parallel \mathrm{e}}T_{\mathrm{e}}\right]_{-L}^{L} &= 5L\Gamma(\pm L)T_{\mathrm{e}}(\pm L) \\ &= \int_{-L}^{L}\left[S_{Q\perp} - S_{\mathrm{n}\perp n_{\mathrm{n}}}E_{\mathrm{iz}} + v_{\parallel \mathrm{e}}\nabla_{\parallel}(nT_{\mathrm{e}}) + \chi_{\mathrm{e}}\nabla_{\parallel}(T_{\mathrm{e}}^{5/2}\nabla_{\parallel}T_{\mathrm{e}})\right]ds,\end{aligned} \tag{23}$$

is satisfied, which describes the total heat balance in the flux tube.

With these constraints, for a given density source strength, heat source strength, and total amount of ionization in the observed flux tube, the refined two-point model, consisting of Eqs. (17,18,20,22), can be solved self-consistently. We compare its results to the set of simulations described in Sec. 3 in Fig. 3. The results from the refined two-point model and the simulations show very good agreement.

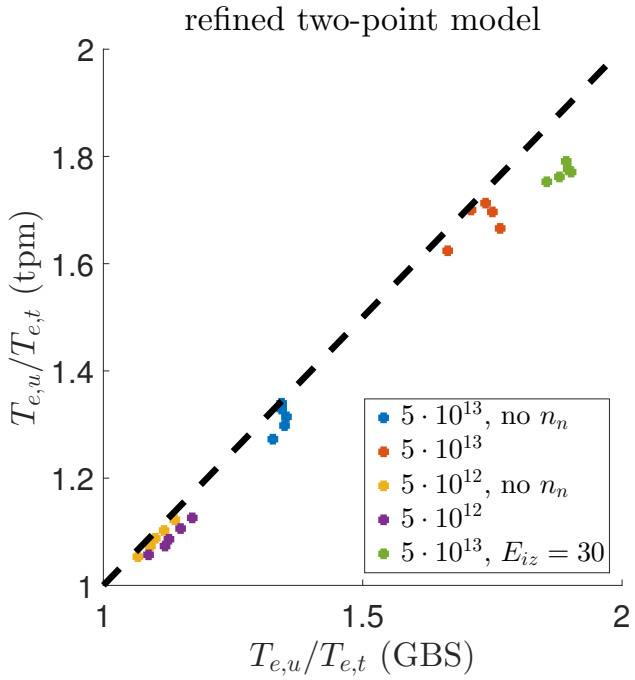

Figure 3: Comparison of the refined two-point model, Eqs. (17-18), with the same set of GBS simulations as used in Fig. 1 and described in Sec. 3.

5 Discussion and conclusions

We test separately the main differences between the simple and the refined two-point model to determine the reason behind the significantly better agreement of the latter with the turbulence simulations. We observe that the shape of the source terms $S_{n\perp}$ and $S_{Q\perp}$ (from constant to a cosine poloidal dependence) does not improve significantly the agreement of the simple two-

point model. However, a significant effect can be observed by including the plasma-neutral interaction terms. This was also observed by Tokar et al. [20], where an improved two-point model is described in which the neutrals are modelled as exponentially decaying from the limiter, similar to the approach in the present paper, including a diffusive model for the charge-exchange processes in addition. However, the inclusion of the pressure gradient term in Eq. (18), $v_{\parallel \mathrm{e}} \nabla_{\parallel} (n T_{\mathrm{e}})$, is even more important. This term originates from the plasma compressibility in the Braginskii equations.

To conclude, taking into account these effects, the refined two-point model that we derived from the drift-reduced Braginskii equations for the limited tokamak SOL predicts the ratio between upstream and target electron temperatures along a flux tube from three input parameters, namely the particle source and heat source to the flux tube due to perpendicular turbulent transport, as well as the ionizations source strength in the flux tube, in very good agreement with GBS turbulence simulations. In particular, the inclusion of plasma-neutral interactions and the additional term in the heat equation are necessary to accurately retrieve the electron temperature ratios observed in turbulent SOL simulations.

In the present paper, we have focused our attention on the electron tem-

perature drop. We would like to remark that evaluating the same drop for the ion temperature brings an additional difficulty. In fact, in the drift-reduced Braginskii equations, Eqs. (3-8), the plasma density and the electron temperature are advected by the electron velocity [see Eq. (3) and Eq. (7)], while the ion temperature is advected by the ion velocity [see Eq. (8)]. The combination of the plasma density and ion temperature equation to an ion heat equation is therefore not straightforward. While $v_{\parallel,i} \approx v_{\parallel,e}$ is a good approximation for the electrons, since it only appears in the term proportional to $\nabla_\parallel j_\parallel$ in the electron temperature equation, Eq. (7), and the other terms in this equation are much larger, it is not a good approximation for the ions. On the other hand, the parallel heat conduction is much smaller for the ions than for the electrons, and can be neglected in most cases.

This paper presents, to our knowledge, the first comparison between a two-point model including plasma-neutral interactions and turbulence simulations of the tokamak SOL. This comparison has ultimately allowed us to develop a more refined two-point model. As progress in the development of three-dimensional turbulence codes evolves, we can foresee improvements of two-point models in more advanced tokamak exhaust configurations.

6 Acknowledgments

The authors acknowledge useful discussions with F. Halpern, J. Loizu, F. Riva, and C. Theiler. Part of the simulations presented herein were carried out using the HELIOS supercomputer system at Computational Simulation Centre of International Fusion Energy Research Centre (IFERC-CSC), Aomori, Japan, under the Broader Approach collaboration between Euratom and Japan, implemented by Fusion for Energy and JAEA; and part were carried out at the Swiss National Supercomputing Centre (CSCS) under Project ID s549. This work has been carried out within the framework of the EUROfusion Consortium and has received funding from the Euratom research and training programme 2014-2018 under grant agreement No 633053. The views and opinions expressed herein do not necessarily reflect those of the European Commission.

References

[1] Akio Arakawa, Computational design for long-term numerical integration of the equations of fluid motion: Two-dimensional incompressible flow. part i, Journal of Computational Physics **1** (1966),

no. 1, 119–143.

[2] S. I. Braginskii, Transport processes in a plasma, Reviews of Plasma Physics **1** (1965), 205.

[3] H. Bufferand, B. Bensiali, J. Bucalossi, G. Ciraolo, P. Genesio, Ph. Ghendrih, Y. Marandet, A. Paredes, F. Schwander, E. Serre, et al., Near wall plasma simulation using penalization technique with the transport code SOLEDGE2D-EIRENE, Journal of Nuclear Materials **438** (2013), S445–S448.

[4] B.D. Dudson, M.V. Umansky, X.Q. Xu, P.B. Snyder, and H.R. Wilson, BOUT++: A framework for parallel plasma fluid simulations, Computer Physics Communications **180** (2009), no. 9, 1467–1480.

[5] Y. Feng, F. Sardei, J. Kisslinger, P. Grigull, K. McCormick, and D. Reiter, 3D edge modeling and island divertor physics, Contributions to Plasma Physics **44** (2004), no. 13, 5769.

[6] F.D. Halpern, P. Ricci, S. Jolliet, J. Loizu, J. Morales, A. Mosetto, F. Musil, F. Riva, T.M. Tran, and C. Wersal, The gbs code for tokamak scrape-off layer simulations, Journal of Computational Physics **315** (2016), 388408.

[7] V Kotov and D Reiter, Two-point analysis of the numerical modelling of detached divertor plasmas, Plasma Phys. Control. Fusion **51** (2009), no. 11, 115002.

[8] Martin Wilhelm Kutta, Beitrag zur näherungsweisen Integration totaler Differentialgleichungen, Zeitschrift für Mathematik und Physik **46** (1901), 435–453.

[9] A Loarte, B Lipschultz, A.S Kukushkin, G.F Matthews, P.C Stangeby, N Asakura, G.F Counsell, G Federici, A Kallenbach, K Krieger, A Mahdavi, V Philipps, D Reiter, J Roth, J Strachan, D Whyte, R Doerner, T Eich, W Fundamenski, A Herrmann, M Fenstermacher, P Ghendrih, M Groth, A Kirschner, S Konoshima, B LaBombard, P Lang, A.W Leonard, P Monier-Garbet, R Neu, H Pacher, B Pegourie, R.A Pitts, S Takamura, J Terry, E Tsitrone, the ITPA Scrape-off Layer, and Diver Group, Chapter 4: Power and particle control, Nuclear Fusion **47** (2007), no. 6, S203–S263.

[10] J. Loizu, P. Ricci, F. D. Halpern, and S. Jolliet, Boundary conditions for plasma fluid models at the magnetic presheath entrance, Phys. Plasmas **19** (2012), no. 12, 122307.

[11] D. Reiter, Progress in two-dimensional plasma edge modelling, Journal of Nuclear Materials **196-198** (1992), 8089.

[12] D. Reiter, M. Baelmans, and P. Börner, The EIRENE and B2-EIRENE codes, Fusion Science and Technology **47** (2005), no. 2, 172–186.

[13] P. Ricci, F. D. Halpern, S. Jolliet, J. Loizu, A. Mosetto, A. Fasoli, I. Furno, and C. Theiler, Simulation of plasma turbulence in scrape-off layer conditions: the GBS code, simulation results and code validation, Plasma Physics and Controlled Fusion **54** (2012), no. 12, 124047.

[14] T. D. Rognlien, J. L. Milovich, M. E. Rensink, and G. D. Porter, A fully implicit, time dependent 2-D fluid code for modeling tokamak edge plasmas, Journal of Nuclear Materials **196-198** (1992), 347351.

[15] R. Schneider, D. Reiter, H. P. Zehrfeld, B. Braams, M. Baelmans, J. Geiger, H. Kastelewicz, J. Neuhauser, and R. Wunderlich, B2-EIRENE simulation of ASDEX and ASDEX-upgrade scrape-off layer plasmas, Journal of Nuclear Materials **196-198** (1992), 810815.

[16] P. Stangeby, The plasma boundary of magnetic fusion devices, IOP Publishing, 2000.

[17] P C Stangeby, A tutorial on some basic aspects of divertor physics, Plasma Phys. Control. Fusion **42** (2000), no. 12B, B271–B291.

[18] Andreas Stegmeir, David Coster, Omar Maj, Klaus Hallatschek, and Karl Lackner, The field line map approach for simulations of magnetically confined plasmas, Computer Physics Communications **198** (2016), 139–153.

[19] P. Tamain, H. Bufferand, G. Ciraolo, C. Colin, D. Galassi, Ph. Ghendrih, F. Schwander, and E. Serre, The TOKAM3x code for edge turbulence fluid simulations of tokamak plasmas in versatile magnetic geometries, Journal of Computational Physics **321** (2016), 606–623.

[20] M. Z. Tokar, M. Kobayashi, and Y. Feng, Improved two-point model for limiter scrape-off layer, Phys. Plasmas **11** (2004), no. 10, 4610.

[21] C. Wersal and P. Ricci, A first-principles self-consistent model of plasma turbulence and kinetic neutral dynamics in the tokamak scrape-off layer, Nuclear Fusion **55** (2015), no. 12, 123014.

[22] A. Zeiler, J. F. Drake, and B. Rogers, Nonlinear reduced Braginskii equations with ion thermal dynamics in toroidal plasma, Phys. Plasmas **4** (1997), no. 6, 2134.